

PHYSICAL REVIEW D

PARTICLES AND FIELDS

THIRD SERIES, VOLUME 31, NUMBER 5

1 MARCH 1985

Production of the $\bar{K}^{*0}(890)$ resonance in π^+p interactions at 16 GeV/c

A. Jawahery,* W. A. Mann, T. Maruyama,[†] and R. H. Milburn
Tufts University, Medford, Massachusetts 02155

J. Hylan[‡] and Z. Ming Ma[§]
Michigan State University, East Lansing, Michigan 48824

P. V. K. S. Baba, Devanand, G. L. Koul, V. K. Gupta, N. K. Rao, and G. Singh
University of Jammu, Jammu 180001, India
(Received 28 September 1984)

The inclusive process $\pi^+ + P \rightarrow \bar{K}^{*0}(890) + X$ is studied at 16 GeV/c using a 2-m streamer chamber containing a central liquid hydrogen target. From photographs triggered by detection of a forward K^- meson, the signal $\bar{K}^{*0} \rightarrow K^- \pi^+$ is extracted. The inclusive rate for \bar{K}^{*0} production into the forward hemisphere $\sigma(x_F > 0.3)$ is $115 \pm 27 \mu\text{b}$; the p_T^2 distribution is found to have a slope constant of $3.3 \pm 0.6 (\text{GeV}/c)^2$. The Feynman- x distribution for \bar{K}^{*0} is consistent with a Kutli-Weisskopf model in which the valence and sea quarks of the incident pion interact with only the sea quarks of the target proton.

INTRODUCTION

The picture of nucleons obtained from study of deep-inelastic scattering of electrons and neutrinos¹ is that they consist of three "valence" quarks (of u and d flavors) together with a "sea" of quark-antiquark pairs ($u\bar{u}$, $d\bar{d}$, $s\bar{s}$, $c\bar{c}$, etc.) bound together with the gluonic quanta of quantum chromodynamics (QCD). This parton interpretation of nucleonic structure, albeit simplistic in terms of current understanding of the deeper aspects of QCD, nonetheless facilitates the classification of production processes according to the flavor content of the initial and final states. Additionally, it provides a framework for the parametrization of experimental data in terms of quark and gluon distribution functions together with fragmentation functions for all mesons and baryons, rather than just for target nucleons.² Extensions of the parton-model picture from the high- p_T regime to low- p_T phenomena have incorporated the Drell-Yan mechanism³ and its generalizations into a variety of processes, including the inclusive production of vector mesons in hadronic interactions.⁴⁻⁷ The essence of these "quark-fusion-model" schemes is that a valence or sea quark from the beam hadron is considered to fuse with a sea antiquark from the target to form an outgoing meson. The model ingredients are simply the incident quark distribution functions which are used to calculate the p_T and x_F distributions of the outgoing meson.

Various incident and outgoing particles may be selected

to help isolate the different distributions of the individual quark flavors in the primary hadrons. To the extent that a self-consistent parametrization of the quark (and gluon) structures of hadrons can be developed in this way, one hopes to clarify the nature of the underlying quark interaction dynamics.

The experimental work reported here concerns the inclusive production reaction $\pi^+(u\bar{d}) + p(uud) \rightarrow \bar{K}^{*0}(s\bar{d}) + X$, in the forward hemisphere at 16 GeV/c, where the valence-quark content of the several particles is as indicated. In a quark-fusion scheme a valence \bar{d} quark in the incident pion may unite with a sea s quark from the proton to produce the observed meson $\bar{K}^{*0}(890)$. This "valence-sea" interaction should reflect the forward momentum carried by the valence quark and be detected preferentially by our trigger-system geometry. Of course, the pion could also contribute an s quark or \bar{d} quark from its sea, and the proton correspondingly a \bar{d} quark or an s quark, but these "sea-sea" interactions would be expected kinematically to be symmetric about $x_F = 0$. Of all the $K^*(890)$ states, the one studied here, $\bar{K}^{*0}(s\bar{d})$ identified by its decay to $\pi^+ K^-$, yields the cleanest (valence-sea) interaction. For example, in one alternative process, $\pi^+(u\bar{d}) + p(uud) \rightarrow K^{*+}(us) + \bar{X}$, the valence u quark can come from either the pion or the proton.

In another process, $\pi^+(u\bar{d}) + p(uud) \rightarrow K^{*0}(d\bar{s}) + X$, the valence quark from the proton carries, on average, a less forward momentum than the valence d quark from the pion in the production of \bar{K}^{*0} and is correspondingly less

resolvable from other interactions symmetric in x_F . As will be later discussed, both the data and the models reflect these qualitative kinematic features.

We report the measurement of $\bar{K}^{*0}(890)$ inclusive production by 16-GeV/c π^+ incident upon a hydrogen target inside the 2-m SLAC streamer chamber, in which the decay to π^+K^- is resolved by downstream Čerenkov and scintillation-counter arrays. A comparison of our results with other experimental data on hadronic $K^*(890)$ production near 16 GeV/c, and with certain quark-fusion models, is included.

APPARATUS

The experimental apparatus, data collection, and processing of streamer-chamber photographs are described in publications⁸⁻¹⁰ and theses.^{11,12} In brief, a beam of 16-GeV/c π^+ mesons at the Stanford Linear Accelerator Center was transported onto a narrow 61-cm-long liquid hydrogen target contained within the sensitive volume of the 2-m SLAC optical streamer-chamber facility.⁸ The magnetic field in the streamer chamber was 13 kG. Negative particles emerging downstream were detected and analyzed in a 100-element "picket-fence" scintillation-hodoscope array to identify tracks of momentum greater than 2.5 GeV/c. These tracks then passed through a 10-cell isobutane-Čerenkov-threshold-detector array and were subsequently vetoed, if their Čerenkov pulse heights indicated that they were either pions of momenta above 2.73 GeV/c or kaons above 9.63 GeV/c (Ref. 9). Signals from the scintillation and Čerenkov arrays were combined in a fast-logic system to generate an electronic trigger signifying the emergence from the interaction of a K^- particle between 2.73 and 9.63 GeV/c. Included in the trigger was a beam-line Čerenkov signal which reduced the K^+ contamination in the beam from 8.1% to 1.5%. The resulting electronic trigger was used to fire the streamer chamber and record the interaction with three-view precision stereo photography. The individual counter signals were latched, the isobutane-Čerenkov-counter signals pulse-height analyzed, and the resulting data recorded on magnetic tape for later correlation with the photographic data and further analysis. Data were also recorded from a second isobutane threshold Čerenkov counter, identical to that used for the trigger but mounted on the "positive" side of the beam.

Film scanning and measurement was carried out by means of image-plane digitizers according to conventional track-chamber procedures, augmented by the requirement that a negative track in the photograph be found to extrapolate to the picket-fence/Čerenkov channel triggering the event. Measurements were processed using the geometry code TVGP followed by a track-extrapolation program APACHE (Ref. 13) which locates the invisible primary event vertex in the hydrogen target. In the sample of acceptable K^- trigger tracks, momenta above 3.0 GeV/c were required; it was estimated that the efficiency of the isobutane-Čerenkov counter in rejecting pions was above 98% (Ref. 9). The final selection of an acceptable K^- was based upon a reextrapolation of the measured candidate track through the magnetic field into the trigger

counter array, and verification that the affected Čerenkov counter had recorded no significant pulse height above its pedestal value for the event epoch in question.

The exposure included about 25×10^6 beam pulses, at 5 to 8 beam particles per pulse. The total number of triggered photographs was about 302 000, yielding 91 rolls of film in 45 days. The work reported here represents the complete analysis of about 8% of the total exposure. However, for the inclusive \bar{K}^{*0} production, the significant features of interest are already evident with this portion of the data, and the statistics are adequate for comparison with other production channels.

Of the 21 800 frames under study, 39% yielded a *bona fide* trigger track. Of these 1044 were rejected for having more than 14 secondary tracks, a category including multiple interactions, upstream and target wall interactions, etc. Acceptable events were also required to extrapolate to a vertex within the target fiducial volume, as located by the APACHE program, which included the trigger track. In about 20% of the final sample, the ambiguity among several possible primary interactions was resolved by using APACHE iteratively in order to achieve single-vertex fits by minimizing χ^2 for the various track combinations including the trigger track. The resulting data set, after imposition of cuts to optimize this process, yielded 3245 fitted events of which 2327 had unique solutions. The cuts included consideration of the overall goodness of fit, the fit to the identified trigger track itself, and the charge balance of the secondary tracks associated with the event in relation to the primary charge of +2 (Ref. 12). Unresolved ambiguities were included with appropriate weighting factors.

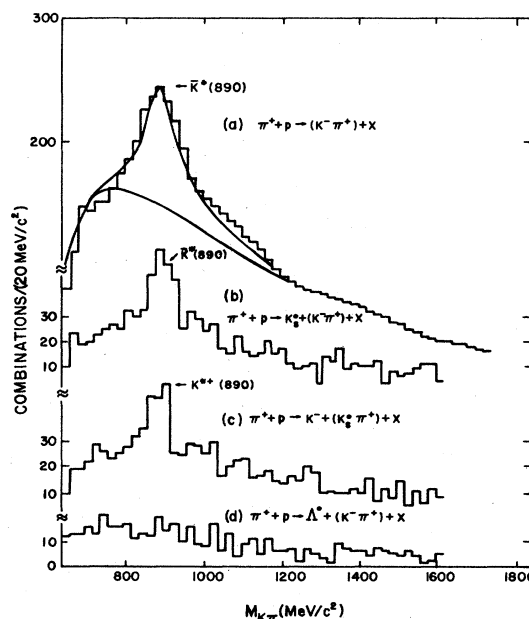


FIG. 1. Invariant-mass distributions of $K\pi$ systems for (a) $\pi^+ + p \rightarrow (K^- \pi^+) + X$ (b) $\pi^+ + p \rightarrow K_s^0 + (K^- \pi^+) + X$, (c) $\pi^+ + p \rightarrow K^- + (K_s^0 \pi^+) + X$, and (d) $\pi^+ + p \rightarrow \Lambda^0 + (K^- \pi^+) + X$. The curves in (a) represent the fits discussed in the text.

ANALYSIS

The present study associates positive secondary tracks, assumed to be π^+ , with the trigger track, identified as K^- . The invariant mass distribution of these combinations is shown in Fig. 1(a). A clear $\bar{K}^{*0}(890)$ resonance is seen. For comparison, Figs. 1(b), 1(c), and 1(d) show the $K\pi$ mass distributions from events with an identified K^- trigger accompanied by visible "vee" decays, as extracted from our earlier study of the entire 302 000-picture exposure.¹² The latter events also show evidence for $\bar{K}_S^0 K^{*0}$ and $K^- K^{*+}$ production ($S=0$), but not for $\Lambda \bar{K}^*$ ($S=-2$), consistently with expectation.

The vee-associated channels are of low statistics and are not used further in this study. A minimum- χ^2 fit to the peak in Fig. 1(a), which uses a Breit-Wigner form together with noninterfering background, is shown by the curve in the figure. The fit gives $M_{\bar{K}^{*0}} = 896 \pm 5$ MeV, $\Gamma = 100 \pm 12$ MeV which is consistent with accepted values 896 MeV and 50 MeV, when the latter are folded with our overall mass resolution, which is ± 50 MeV. A small subset of the pion candidates in Fig. 1(a) had momentum greater than 3 GeV/c and also passed through the positive-side Čerenkov detector and thus could be identified specifically as π^+ . These are shown in Fig. 2(b).

The geometrical acceptance for detecting a K^- trigger track from $\bar{K}^{*0} \rightarrow K^- + \pi^+$ was calculated as a function of transverse momentum p_T^2 and Feynman x parameter (x_F) assuming (a) the differential \bar{K}^{*0} production cross section factors according to

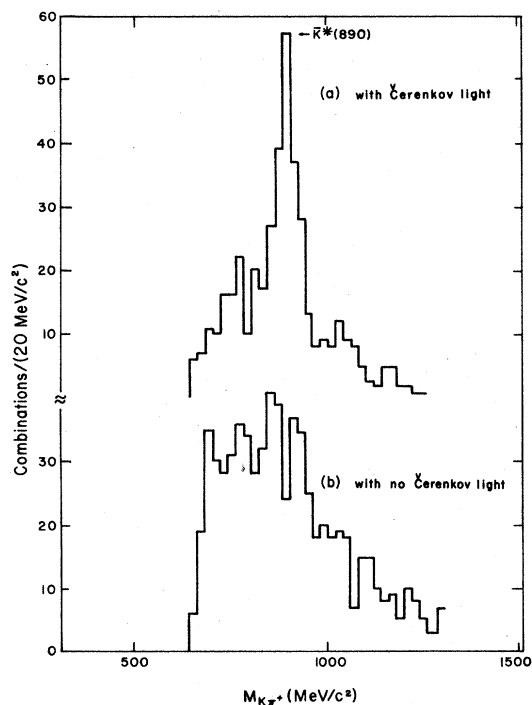


FIG. 2. Invariant-mass distributions for $K^- \pi^+$ for positive tracks extrapolating through the Čerenkov detector with momentum above pion threshold. (a) With Čerenkov pulse, (b) with no Čerenkov pulse.

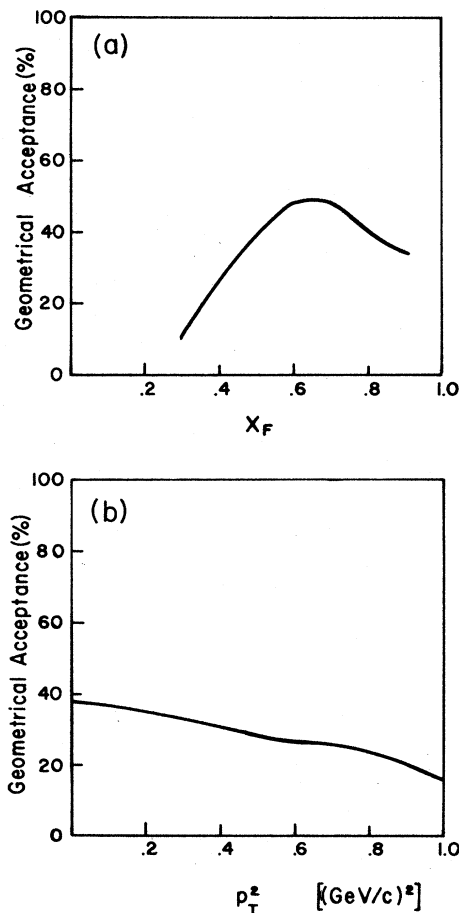


FIG. 3. Geometrical-acceptance functions for $\bar{K}^{*0}(890)$ detection. (a) As a function of $x_F = 2p_{\text{long}}/\sqrt{s}$, (b) as a function of p_T^2 .

$$f(x_F) \exp(-B p_T^2),$$

(b) the parameter $B = 3.5 (\text{GeV}/c)^{-2}$, and (c) the \bar{K}^{*0} decays isotropically in its rest frame. The geometrical acceptances were found to be insensitive to the value of the slope parameter B actually used. With these assumptions, \bar{K}^{*0} decays were generated for fixed x_F values in the range 0.0–0.9, and the acceptance was determined by extrapolating the K^- decay product into the hodoscope region to see whether it would have triggered a photograph. The resulting acceptance as a function of x_F , shown in Fig. 3(a), is used to correct the observed frequencies of \bar{K}^{*0} production. The acceptance-corrected distribution in x_F was then used as input in a further simulation, for p_T^2 between 0.0 and 1.0, to establish similarly the geometrical trigger acceptance as a function of p_T^2 . This is shown in Fig. 3(b). The p_T^2 distribution of \bar{K}^{*0} production, before and after acceptance corrections, is shown in Fig. 4. The final distribution is fitted to a slope parameter $B = 3.3 \pm 0.6 (\text{GeV}/c)^{-2}$ which is consistent with the initial assumption of 3.5 and with other measurements in this energy range.¹⁴ The choice of initial B was not critical to the results from this procedure. The x_F distribu-

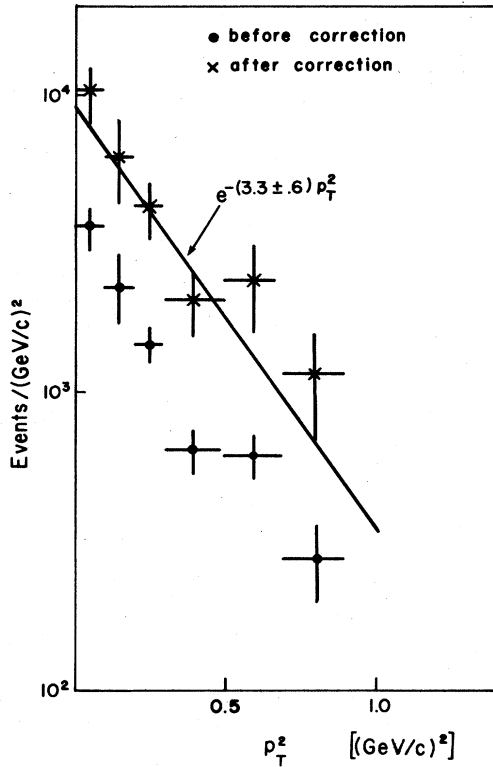


FIG. 4. Distribution in p_T^2 for $\bar{K}^{*0}(890)$ inclusive production, before and after acceptance correction. The fitted curve is for slope parameter 3.3 ± 0.6 $(\text{GeV}/c)^{-2}$.

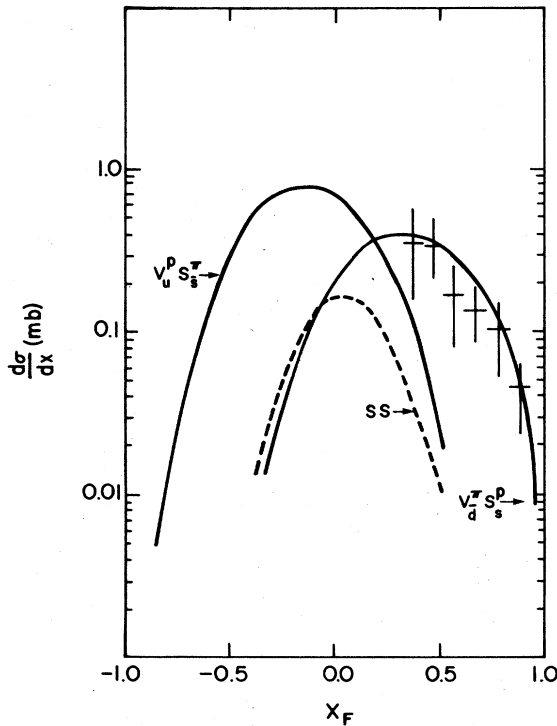


FIG. 5. Distribution in $x_F = 2p_{\text{long}}/\sqrt{s}$ for $\bar{K}^{*0}(890)$ inclusive production. The curves are the predictions of Kinnunen (Ref. 7) for the indicated processes.

tion of the \bar{K}^{*0} production, with an estimated 953 ± 35 events, is corrected by the acceptance function of Fig. 3(a), and also for invisible decay modes. This leads to an estimated inclusive cross section for this process with $x_F > 0.3$ of $115 \pm 27 \mu\text{b}$, distributed in x_F as shown in Fig. 5.

RESULTS

In Fig. 5 we include phenomenological curves depicting the parametrization of Kinnunen⁷ based upon the Kuti-Weisskopf model^{4,5} and quark counting rules. The curve $V^\pi S^P$ is for the production of the $(\bar{s}d)$ \bar{K}^{*0} with the valence \bar{d} quark from the incident π^+ distributed as

$$V_d^\pi(x) = (0.75)(1-x)/\sqrt{x} \tag{1}$$

and the s quark from the struck proton sea as

$$S_s^P(x) = \lambda_s(0.36)(1-x)^7/x \tag{2}$$

It closely resembles the data. Here $\lambda_s = 0.43$ is the strange-quark suppression factor in the proton sea. Also shown in Fig. 5, are predicted x_F dependences for sea-sea interactions alone, and for $V^P S^\pi$ where the proton contributes the valence u quark as in $\pi^+ p \rightarrow K^{*+} + X$. Unfortunately, this process also permits the valence u quark to come from the incident π^+ which obscures the x_F dependence of the production. In the present data, as Fig. 5 shows, the cross section falls off sharply in the forward direction but remains significant in a region where

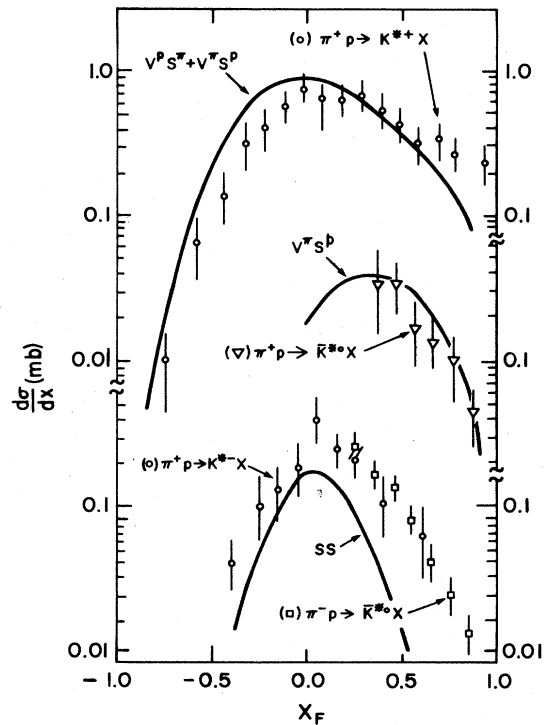


FIG. 6. Comparison of inclusive K^* production by $\pi+p$ at 16 GeV/c in various charge states; the x_F distributions adapted from Kinnunen (Ref. 7) are shown superimposed on data from Refs. 14 and 17, and from the present work.

the contribution from pion sea quarks is expected to be negligible. Of the various channels for the process $\pi^+p \rightarrow (K^*, \bar{K}^*)^{+-0} + X$, the one studied in the present experiment gives the cleanest resolution of the valence-quark contribution. A synoptic picture of the present experimental situation for inclusive K^* production by pions at 15–16 GeV, with Kinnunen's parametrizations superimposed, is shown in Fig. 6.

DISCUSSION

As illustrated in Fig. 6, the inclusive production of $K^*(890)$ states by pions incident on protons at 15–16 GeV/c can be interpreted self-consistently in terms of a parton-model parametrization such as Kinnunen's.⁷ The new data we provide are unique in that they distinguish the specific effect of a single valence quark in the primary pion striking, in this simplified picture, a strange quark in the proton sea.

The work of Kinnunen⁷ utilized the protonic quark

structure functions of a Kuti-Weisskopf model⁴ as modified by McElhaney and Tuan.⁵ These modified structure functions have stood up well.¹⁵ Kinnunen's structure functions for the pion are based upon a Kuti-Weisskopf model with several phenomenological arguments.¹⁶ From the work reported here (Fig. 5) we conclude that Kinnunen's proposed structure function [Eq. (1)] for valence \bar{d} quarks in charged pions is consistent with observation in the region of $x_F = 0.3-0.9$.

ACKNOWLEDGMENTS

This work was supported in part by the U.S. Department of Energy through Contracts Nos. DE-AC02-83ER40085 (Tufts University) and DE-AC02-77ER14529 (Michigan State University). We are indebted to R. Mozley, K. Bunnell, and A. Odian at SLAC, to C. C. Chang and R. Thornton at Tufts, and to K. Blakkan, G. Denison, M. Ghods, and V. Whitelaw at MSU for their valuable assistance during the course of this experiment.

*Present address: Syracuse University, Syracuse, NY 13210.

†Present address: University of Wisconsin, Madison, WI 53706.

‡Present address: John Hopkins University, Baltimore, MD 21218.

§Present address: Bell Laboratories, Murray Hill, NJ 07974.

¹See, for example, Secs. I and II of R. D. Field and R. P. Feynman, Phys. Rev. D **15**, 2590 (1977).

²V. Barger and R. J. N. Phillips, Nucl. Phys. **B73**, 269 (1974).

³S. D. Drell and T. M. Yan, Phys. Rev. Lett. **25**, 316 (1970).

⁴J. Kuti and V. F. Weisskopf, Phys. Rev. D **4**, 3418 (1971).

⁵R. McElhaney and S. F. Tuan, Phys. Rev. D **8**, 2267 (1973).

⁶S. Nandi, V. Rittenberg, and H. R. Schneider, Phys. Rev. D **17**, 1336 (1978).

⁷R. Kinnunen, University of Helsinki Report Series in Physics HU-P-178, 1980 (unpublished). The full set of structure functions, in addition to $V_d^\pi(x)$ of Eq. (1) and S_s^p of Eq. (2), includes

$$S_{u,u}^p(x) = S_{d,\bar{d}}^p(x) = S_s^p(x)/\lambda_s = S_s^p(x)/\lambda_x,$$

$$V_{u,u}^\pi(x) = V_{d,\bar{d}}^\pi(x),$$

$$V_d^\pi(x) = 1.1(1-x)^{3.1}/\sqrt{x},$$

$$V_s^\pi(x) = 1.79(1+2.3x)(1-x)^3/\sqrt{x},$$

and

$$\begin{aligned} S_{u,u}^\pi(x) &= S_{d,\bar{d}}^\pi(x) = S_{s,s}^\pi(x)/\lambda_s \\ &= 0.30(1-x)^5/\sqrt{x}. \end{aligned}$$

⁸C. del Papa, Phys. Rev. D **13**, 2934 (1976).

⁹J. Hylan *et al.*, Nucl. Instrum. Methods **185**, 107 (1981).

¹⁰J. Hylan *et al.*, Phys. Rev. D **27**, 1439 (1983).

¹¹J. E. Hylan, Ph.D. dissertation, Michigan State University, 1982.

¹²A. Jawahery, Ph.D. dissertation, Tufts University, 1981.

¹³A. Seiden, Ph.D. dissertation, University of California, Santa Cruz, 1975. APACHE extrapolates selected track subsets to find a track vertex and then repeats the TVGP fit using it, continuing until goodness-of-fit criteria are met. In the present study the triggering K^- track was required to be among the included tracks for an acceptable vertex.

¹⁴K. Bockmann *et al.*, Nucl. Phys. **B166**, 284 (1980), Table 3.

¹⁵H. Deden *et al.*, Nucl. Phys. **B85**, 269 (1975).

¹⁶V. V. Kniazev *et al.*, Report No. OT0-77-106, Serpukhov, 1977 (unpublished).

¹⁷C. Evangelista *et al.*, Phys. Lett. **70B**, 373 (1977).